Available online at: http://www.ijmtst.com/vol4issue10.html

International Journal for Modern Trends in Science and Technology

ISSN: 2455-3778 :: Volume: 04, Issue No: 10, October 2018

Estimation of Evapotranspiration using Landsat 8 Satellite Images and SEBAL Method

Mohammad Hamed Saeefar[1] | Bohlol Alijani[2]

[1]Ph.D. Student in Climatology, Department of geography, Kharazmi University, Tehran, Iran
[2]Professor in Climatology, Kharazmi University, Tehran, Iran

To Cite this Article
Mohammad Hamed Saeefar and Bohlol Alijani, "Estimation of Evapotranspiration using Landsat 8 Satellite Images and SEBAL Method", *International Journal for Modern Trends in Science and Technology*, Vol. 04, Issue 10, October 2018, pp.-07-14.

Article Info
Received on 03-Aug-2018, Revised on 12-Sept-2018, Accepted on 05-Oct-2018.

ABSTRACT

Today remote sensing is used in various sciences such as geography, biology, meteorology, agriculture, water resources management, etc. Therefore, using the algorithms available in the remote sensing of evapotranspiration, one can take a major step in the management of water resource swhich is included SEBAL algorithm.In this study, using this algorithm, multi-spectral satellite data and meteorological data such as temperature, duration of sunshine, wind, saturation vapor pressure, soil moisture and so on were used to calculate surface albedo, surface temperature and vegetation status index. Seasonal monitoring of evapotranspiration changes over the past two years has shown that the process of evapotranspiration changes during a year is periodic that start at the beginning of the year (as in the picture of January 2018 and February 2017) with a relatively low amount, then it has an uptrend to reach its highest levels in the summer (July 2016 and 2017), and then it has downward trend and at the end of the year (October 2016 and 2017) reaches its minimum value. The highest amount of evapotranspiration dates to the 7th month of every year, which is the summer season. Due to the fact that the temperature of evapotranspiration in the heat season is higher because of high air temperature and atmospheric conditions, the results confirm the accuracy of this subject that highest amount of evapotranspiration is in the 7th month of every year.

KEYWORDS: *Evapotranspiration, SEBAL algorithm, Landsat 8 satellite images, Meteorological stations*

I. INTRODUCTION

Increasing demand for water due to the need to produce more food emphasizes the need for planning for agricultural water issues. With proper irrigation planning and determining the time and rate of irrigation, the water needed for the plant is provided, and in addition to unnecessary consumption of water, the effects of drought stress and yield reduction are prevented [1].

On the other hand, due to the warming of the air and the increase dryness in warm and dry seasons, especially in areas such as Iran, there is the possibility of fire of pastures and forests. Knowledge of time, dispersion and water stresses on trees and pastures in warm and dry seasons are also important reasons for measuring water stress and soil moisture content [2]. Now, with the development of remote sensing technology, soil moisture estimationhas been directly or indirectly taken into consideration by researchers. When the adaptation between the sensor data and the

measured properties of the soil and the plant takes place, it can be concluded about the conditions of a wider area where no real ground measurements have been made [3]. This action leads to the achievement of a true value of remote sensing;it means the ability to obtain very large information with the least number of labors and at a very short time. Therefore, in order to manage the water requirement in large farms and gardens, increase the yield and quality of products, and alsopredict the fire in pastures and forests in warm and dry seasons, the monitoring of the water stress of plants is required using remote sensing technology [4].

Traditional methods in soil moisture field measurements are not desirably able to provide spatial and temporal changes in soil moisture and are not practically possible at basin level. Satellite data is continuously and widely available and provides a wide range of environmental phenomena in space, compared with point situations such as meteorological stations [5].

This capability makes satellite images useful for monitoring moisture. Precise soil moisture determination is a key factor in these studies. Changes in factors such as soil texture, topography, vegetation and irrigation methods make the soil moisture change much time-dependent. Evapotranspiration is one of the important factors in the hydrological cycle and is one of the determinants of energy equilibrium on the ground and water balance and its estimation is required in various fields such as hydrology, agriculture, forest management and pasture management, and water resources management [6]. Remote sensing is one of the new techniques that can be used to estimate evapotranspiration in an area without having to know the background in relation to soil conditions, crop management and farm management [7].

Energy balance methods based on the calculation of evapotranspiration is one of the components of the energy balance equation. SEBAL algorithm (earth's energy balance) is one of the most important and most widely used energy balance methods for estimating real evapotranspiration using remote sensing data based on experimental and physical relationships.SEBAL algorithm is a method that estimates the actual evapotranspiration with minimum ground data and this algorithm was first presented by Bastiaanssen et al. 1998 [8, 9]. This algorithm was reformed in 2002 by Allen et al., that the new modified algorithm is very similar to the METRIC energy balance algorithm presented by Allen et al. (2007). [10] So far, many studies have been conducted that all indicate the effectiveness of the SEBAL method for estimating real evapotranspiration in a regional scale and large basins [11, 12, 13]. Nori (2009) conducted a research and investigated the use of the SEBAL algorithm for calculating real evapotranspiration using MODIS sensor images under catchment area (the Mashhad in Iran). The results showed that the MODIS sensor images and SEBAL algorithm are able to accurately estimate the actual evapotranspiration on a daily scale in Mashhad.

Sanein Nejad and et al. [14] also estimated the amount of evapotranspiration using MODIS sensor images for three days of the year and in a region in Mashhad. The results of this study showed that the images of MODIS and SEBAL algorithm have a good ability to estimate the actual evapotranspiration on a daily scale. Pourmohammadi et al. [15] determined and zoned the amount of real evapotranspiration by using MODIS images and SEBAL algorithm in one region of Yazd province. The results of this study, while showing the spatial variations of evapotranspiration from different land uses, reflect the significant changes in this factor in different basin uses. Sun et al. [16] and Jia et al. [15] estimated the amount of evapotranspiration using the SEBAL method and using the images of MODIS and Landsat, respectively, in two regions of China, and showed that the application of the algorithm SEBAL can play an important role in water resources decision making. Therefore, according to the importance of water in the country and the necessity of controlling water consumption and prevention of waste of water, in this study, the amount of evapotranspiration in the city of Ahvaz and the suburbs is estimated using Landsat 8 satellite images and SEBAL method.

II. METHODOLOGY

2.1 The studied area and data:

The studied area is located in the city of Ahvaz and the suburbs that is located in the geographic coordinate system with a longitude of 31 ° 44'31.13 "N and latitude 49 ° 19'08.29" E (figure 1). In this study, a series of eight Landsat 8 satellite images have been used seasonally since the past 2 years.

Figure 1 The studied area

To calculate evapotranspiration, a map of the digital terrain model of land is needed, which is provided by https://earthexplorer.usgs.gov/. Also, the needed meteorological information is obtained from the weather stations of the cities in the region such as Ahvaz and Shushtar, etc. that are available on the Iranian meteorological site.

The purpose of this study is to obtain the instantaneous evapotranspiration changes in the past two years in a seasonal manner. To achieve this goal, first, the evapotranspiration for each of the 8 Landsat 8 satellite images is downloaded from the https://earthexplorer.usgs.gov/ site. Subsequently, an initial pre-processing with ENVI software was performed on the downloaded photographs from the site.

In this study, SEBAL algorithm was used to estimate evapotranspiration. SEBAL is an image processing model that calculates evapotranspiration and other energy transformations in the ground surface using digital image data that is obtained by remote sensing satellites that measure visible radiation, near infraredradiation and thermal infrared radiation.

SEBAL algorithm provides a complete balance of radiation and energy levels along with tangible heat flow and aerodynamic roughness of surfaces. Evapotranspiration is calculated as a fraction of the energy per pixel.

$$\lambda ET = Rn - G - H \quad (1)$$

Where λET is the insensible-heat flux (the energy used to evaporate water), Rn is the pure radiation at the surface (W / m2), G is the heat flux of soil (W / m2), H is the sensible-heat fluxinto the air (W / m2).

Calculation of pure radiation (Rn)

The pure radiation flux at the surface of the earth is achieved using all the inlet and outlet radiation fluxes. The amount of pure radiation on the earth's surface and its components is determined by the following equation.

$$Rn = (1 - \alpha)R_{s\downarrow} + R_{l\downarrow} - R_{l\uparrow} - (1 - \varepsilon_0)R_{l\downarrow} \quad (2)$$

In thisequation, α is the surface albedo; $\varepsilon_0$is the surface emissivity; $R_{s\downarrow}$ is the input shortwave radiation, $R_{l\downarrow}$is the input longwave radiation and $R_{l\uparrow}$is the outputlongwave radiation.

Calculation of the input shortwave radiation ($R_{s\downarrow}$)

The solar radiation flux is direct and diffuse that really reaches to the ground. Assuming smooth sky conditions, solar radiation flux can be calculated for imaging time using the following equation.

$$R_{s\downarrow} = G_{sc} * \cos\theta * d_r * \tau_{sw} \quad (3)$$

That in this equation G_{sc} is the solar constant (1367 W / m2), θ is the Zenith angle, d_r is the inverse of the square of the relative distance Earth-Sun, τ_{sw} is atmospheric transparency. The values of $R_{s\downarrow}$ vary from 200 to 1000 watts per square meter (W/m2), depending on the location and time of the imaging.

Calculate the Zenith angle (θ)

The Zenith angle (θ) is calculated using the date and time of taking satellite images.

Calculation of inverse of the square of the relative distance Earth-Sun d_r

The following equation is used to calculate d_r.

$$d_r = 1 + 0.0033 * \cos\left(DOY\frac{2\pi}{365}\right) \quad (4)$$

DOY is the day of the year according to Julian's calendar

Calculate atmospheric transparency τ_{sw}

To calculate atmospheric transparency, the following equation is used that depends on the elevation of the area.

$$\tau_{sw} = 0.75 + 2 * 10^{-5} * z \quad (5)$$

That in this equation z is the height from the sea level in meters.

Calculation of the input longwave radiation ($R_{l\downarrow}$)

This radiation is the heat flux from the atmosphere to the bottom, which was calculated using the Stefan-Boltzmann equation

$$R_{L\downarrow} = \varepsilon_a \sigma T_a^4 \quad (6)$$

That in this equation ε_a is the atmospheric emissivity, T_a is the temperature near the surface (K), σ is the Stefan-Boltzmann constant with the value of 5.67 * 10-8 W / m2 / K4. The values of $R_{s\downarrow}$vary from 200 to 500 watts per square meter (W/m2), depending on the location and time of the imaging.

Calculation of the output longwave radiation ($R_{l\uparrow}$)

The output longwave radiation was calculated using the Stefan-Boltzmann equation as follows.

$$R_{l\uparrow} = \varepsilon_0 \sigma T_s^4 \quad (7)$$

In this equationε_0 is the atmospheric emissivity, T_s is the surface temperature (K), σ is the Stefan-Boltzmann constant with the value of 5.67*10-8 W/m2/K4. The values of the output longwave radiationvary from 200 to 700 watts per square meter (W/m2), depending on the location and time of the imaging.

Calculation of soil heat flux (G)

Soil heat flux is the amount of heat stored in the soil and vegetation due to molecular guidance. Soil heat flux was calculated using the following experimental relationship developed by Bostansin.

$$\frac{G}{R_n} = \frac{T_s}{\alpha}[0.0032\,\alpha + 0.0062\,\alpha^2] * [1 - 0.978 * NDVI^4] \quad (8)$$

That in this equation$T_s$is the surface temperature in Celsius, α is surface albedo, and NDVI is normalized difference vegetation index.

Calculation of sensible-heat flux (H)

Finally, the sensible-heat flux, which is the amount of heat lost to the air by the convective current and the molecular conductivity due to the temperature difference, is calculated using the following equation for heat transfer.

$$H = \frac{\rho . C_p . dT}{r_{ah}} \quad (9)$$

Where ρ is the density of air (kg / m3), $C_p$is special heat (1004J / kg / K), d_T is thetemperature difference between two heights (z_1,z_2) in degrees Kelvin and $r_{ah}$is aerodynamic resistance for heat transfer (s / m).$z_1$is the exactlyheight of the displacement of the zero level for the surface or vegetation, z_2 is slightly above the zero displacement level. In SEBAL, values of 0.1 for z_1 and 2 meters for z_2 are considered.

The SEBAL model uses two pixel indicators to determine boundary conditions in the energy balance equation.

These two index pixels are called "hot and cold pixels" and are studied in the area.Cold pixels are selected from fully irrigatedfarms, full-vegetation farms, where surface temperatures and air temperatures near the surface are assumed to be equal, and hot pixels are chosen from without vegetation and dry land. Evapotranspiration of plant is considered ETr1.05due to convection. The reference evapotranspiration is calculated from the Penman-Monteithequation, then ET = Rn-G-1.05ETr. The hot pixel is where there is no evapotranspiration and H = Rn-G. Distinguish between hot pixels and cold pixels are difficult to choose from the choice of pixels, because, according to the temperature, many pixels are considered for hot pixels.

In the cool pixel, the sensible heat flux is calculated from the following equation.

$$H_{cold} = Rn - G - \lambda ET_{cold} \quad (10)$$

Based on the experience gained in the state of Idaho, evapotranspiration is about 5% higher than the evapotranspiration of the reference plant in the cool pixel. As a result,ET_{cold} can be assumed to be ETr1.05. Therefore, H_{cold} is calculated from the equation $H_{cold} = Rn - G - 1.05\,\lambda ET_r$. dT_{cold} is also obtained from the following equation.

$$dT_{cold} = \frac{H_{cold} * r_{ah-cold}}{\rho_{cold} * c_p} \quad (11)$$

In the hot pixel, the sensible heat flux is calculated from the following equation.

$$H_{hot} = Rn - G - \lambda ET_{hot} \quad (12)$$

$ET_{hot}$is assumed to be zero for a hot pixel that is selected from non-vegetable fields with a dry soil layer. The sensible heat flux in the hot pixel is calculated from the following equation.

$$dT_{hot} = \frac{H_{hot} * r_{ah-hot}}{\rho_{hot} * c_p} \quad (13)$$

Using the correlation coefficients between the points of the coefficients a and b, the formula is calculated.

$$dT = a + b * T_s \quad (14)$$

The final corrected values for each sensible heat flux per pixel are calculated and used in the energy balance equation to calculate the instantaneous evapotranspiration for each pixel.

III. Discussion and Results

First, photos taken with the Landsat 8 satellite for evapotranspiration in the studied area were downloaded at https://earthexplorer.usgs.gov/.

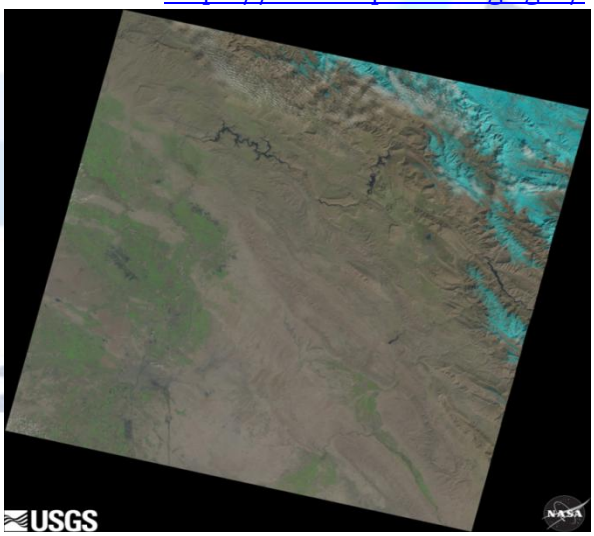

Figure 1Downloadedsample of Landsat 8 satellite image

Preprocessing

Satellite images taken for use require radiometric and atmospheric corrections. The radiometric calibration section in the ENVI software is used to radiometric correction and the FLAASH section in

the ENVI software is used to correct the atmospheric atmosphere. After applying radiometric corrections, the radiance image is obtained (figure 2).

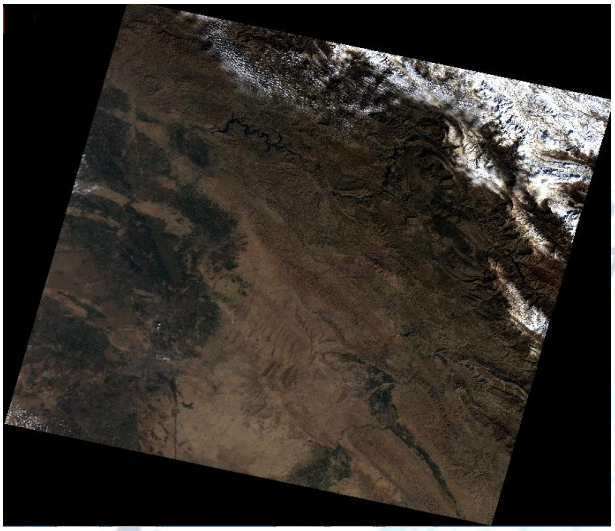

Figure 2 Radian images after preprocessing

After applying the atmospheric correction, the reflectance image is obtained that the reflection of the band 1 is shown in the following figure. After applying the above corrections, the corrected images are ready for use in the next steps to extract evapotranspiration (figure 3).

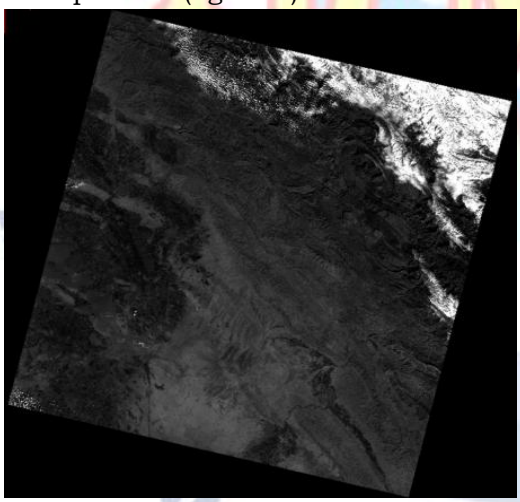

Figure 3 Reflectance images after applying atmospheric correction

SEBAL algorithm

The main parameters for estimating evapotranspiration are Rn, G and H.

Pure Radiation (Rn)

In order to obtain pure radiation, according to equation (2), the albedo parameters, surface emissivity, the input shortwave radiation, the inputlongwave radiation and the output longwave radiation are required, each of which is given below.

Surface emissivity is a function of the leaf area index (LAI), which is calculated using soil-adjusted vegetation index (SAVI). In the following figure, the results of the LAI indices and the final image of surface emissivity are shown.

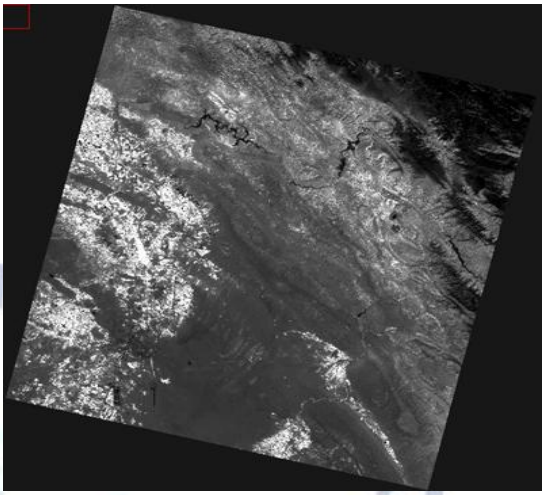

(a)

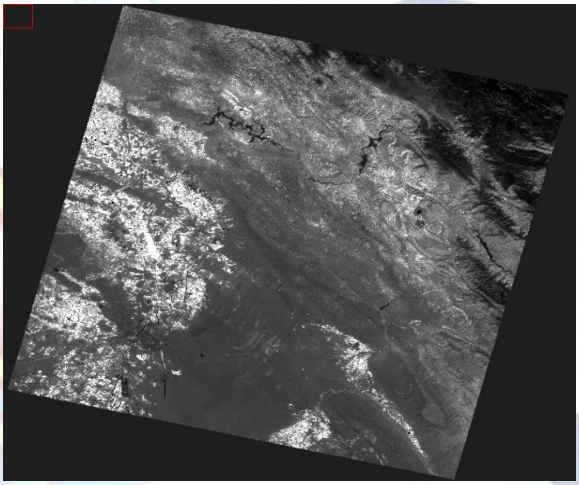

(b)

Figure 4(a) Results of indices of LAI and (b)final image of surface emissivity

Albedo is the percentage of solar radiation reflected by the earth, which is calculated as a weightedtotal of the reflectance of the bands 1 to 7 of Landsat 8. The result of this weightedtotal is as follows (figure 5).

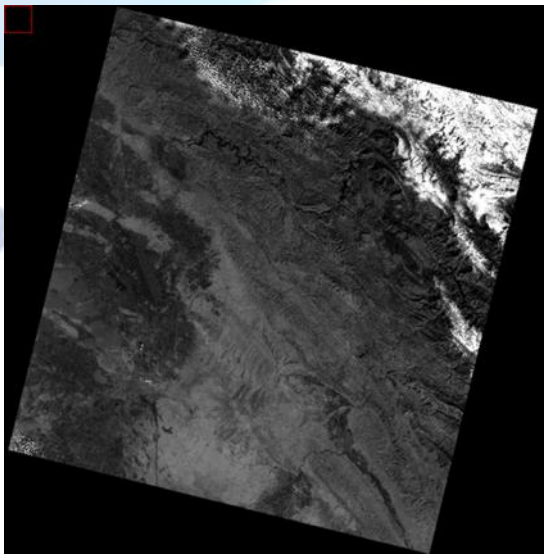

Figure 5 Percentage of reflection of solar radiation by the earth

The results of the input shortwave radiation

The input shortwave radiation is calculated according to equation 3 that atmospheric transparency and dr is required. dr is the reciprocal of the inverse of the square of the relative distance Earth-Sun, DOY is needed due to its equation. In figure 6, DOY different days of the year are shown in the Julian calendar.

Julian Date Calender
(PERPETUAL)

Day	Jan	Feb	Mar	Apr	May	Jun	Jul	Aug	Sep	Oct	Nov	Dec	Day
1	001	032	060	091	121	152	182	213	244	274	305	335	1
2	002	033	061	092	122	153	183	214	245	275	306	336	2
3	003	034	062	093	123	154	184	215	246	276	307	337	3
4	004	035	063	094	124	155	185	216	247	277	308	338	4
5	005	036	064	095	125	156	186	217	248	278	309	339	5
6	006	037	065	096	126	157	187	218	249	279	310	340	6
7	007	038	066	097	127	158	188	219	250	280	311	341	7
8	008	039	067	098	128	159	189	220	251	281	312	342	8
9	009	040	068	099	129	160	190	221	252	282	313	343	9
10	010	041	069	100	130	161	191	222	253	283	314	344	10
11	011	042	070	101	131	162	192	223	254	284	315	345	11
12	012	043	071	102	132	163	193	224	255	285	316	346	12
13	013	044	072	103	133	164	194	225	256	286	317	347	13
14	014	045	073	104	134	165	195	226	257	287	318	348	14
15	015	046	074	105	135	166	196	227	258	288	319	349	15
16	016	047	075	106	136	167	197	228	259	289	320	350	16
17	017	048	076	107	137	168	198	229	260	290	321	351	17
18	018	049	077	108	138	169	199	230	261	291	322	352	18
19	019	050	078	109	139	170	200	231	262	292	323	353	19
20	020	051	079	110	140	171	201	232	263	293	324	354	20
21	021	052	080	111	141	172	202	233	264	294	235	255	21
22	022	053	081	112	142	173	203	234	265	295	326	356	22
23	023	054	082	113	143	174	204	235	266	296	327	357	23
24	024	055	083	114	144	175	205	236	267	297	328	358	24
25	025	056	084	115	145	176	206	237	268	298	329	359	25
26	026	057	085	116	146	177	207	238	269	299	330	360	26
27	027	058	086	117	147	178	208	239	270	300	331	361	27
28	028	059	087	118	148	179	209	240	271	301	332	362	28
29	029		088	119	149	180	210	241	272	302	333	363	29
30	030		089	120	150	181	211	242	273	303	334	364	30
31	031		090		151		212	243		304		365	31

Figure 6 DOY different days of the year

After calculating atmospheric transparency and other parameters, the input shortwave radiation is obtained.

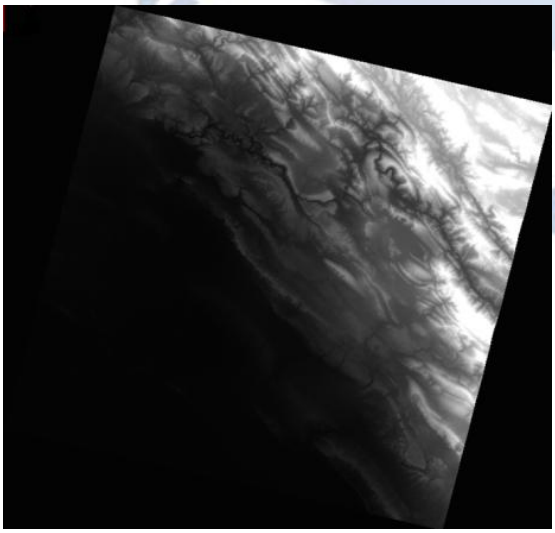

Figure 7 The image of the input shortwave radiation

The output longwave radiation

Due to the fact that the LST map prepared with the thermal bonding 11 has a higher accuracy than the thermal bond 10, Landsat 8 was used to calculate the ground temperature. After calculating the temperature of the surface of the earth and the surface emissivity of the output longwave radiation is obtained (8).

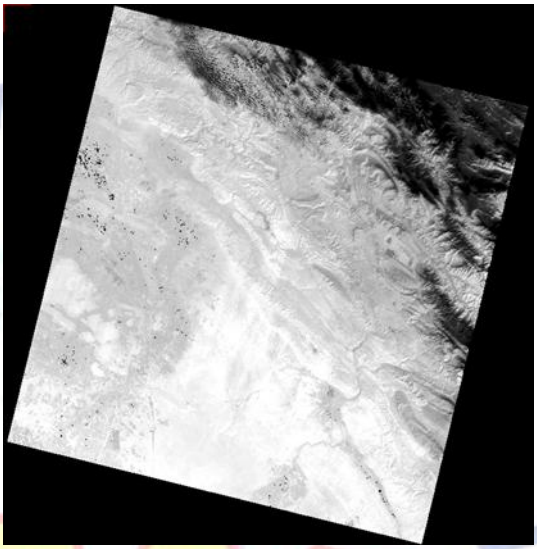

Figure 8 The surface image of output longwave radiation

The input longwave radiation

The near-surface temperature has a linear relationship with the surface temperature, which is calculated using weather station data.Relatively humidityis also required toSurface emissivity calculations obtained from the Meteorological Organization data.

By calculating the parameters mentioned above, the input longwave radiation was obtained (figure9).

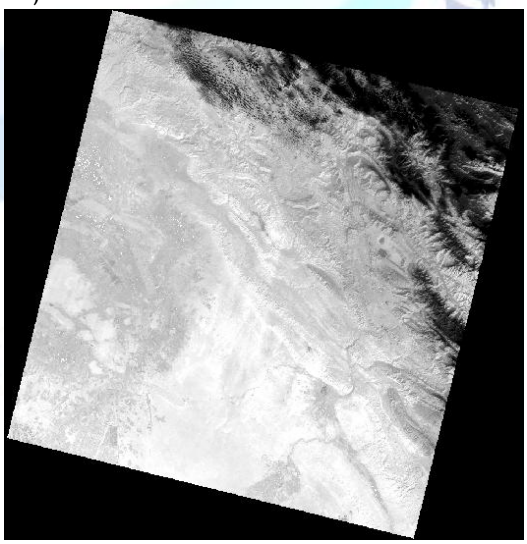

Figure 9 –The image ofinput longwave radiation

After calculating parameters of the input shortwave radiation, the input longwave radiation andoutputlongwave radiation, pure radiation were

calculated. The figure below shows the pure radiation image (figure 10).

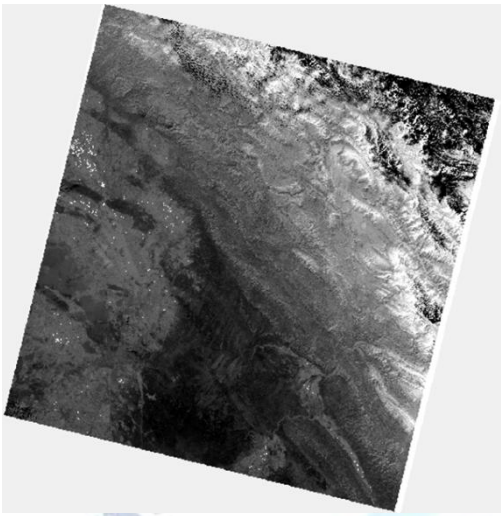

Figure 10 Image of pure radiation

Soil heat flux depends on the surface temperature parameters, albedo, the normalized difference vegetation index (NDVI) and pure radiation index and pure radiation. To calculate this heat flux, the ratio of soil heat flux to pure radiation was used.

To calculate the temperature difference and the aerodynamic resistance, a rotational process was conducted and the values at each step were approached to their correct valuesby updating. The beginning of this process begins by determining the hot and cold pixels, and after reaching the required precision, the cycle is completed and the most appropriate amount of the heat flux is obtained, as shown in the below figure (figure 11).

Figure 11 The image of sensible heat flux

After obtaining the main parameters of the SEBAL algorithm, the hidden heat flux (λET) was estimated. In the end, the rate ofinstantaneous evapotranspiration is calculated as a coefficient of the hidden heat flux and is shown in the below figure (figure 12).

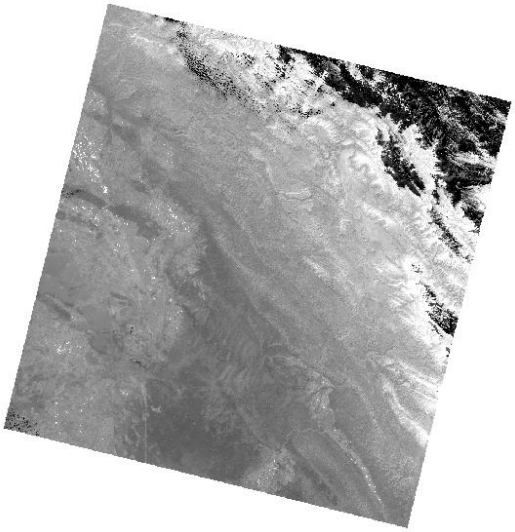

Figure 12 Instantaneous Evapotranspiration

IV. Conclusion

In this study, after obtaining seasonal evapotranspiration from July 2016 for two months, the following changes are obtained.

As shown in the following chart, a similar process has been achieved in the same chapters. According to the chart, the maximum amount of evapotranspiration is in the 7th month, which is the summer season;Because of this fact that the temperature of evapotranspiration in the heat season is higher and high atmospheric conditions that the obtained results confirm the accuracy of this fact.In order to better illustrate the range of evapotranspiration values of the area, in the belowchart, in addition to the mean values, the confidence interval and range of the evapotranspiration of satellite images is shown.

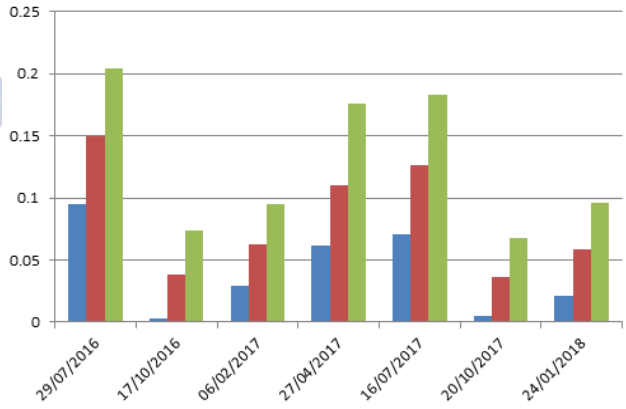

Figure 13 Range of evapotranspiration values of the area

As shown in the chart, process of evapotranspiration changes during a year is periodic that start at the beginning of the year (as in the picture of January 2018 and February 2017) with a relatively low amount, then it has an uptrend to reach its highest levels in the summer (July 2016 and 2017), and then it has downward trend and at the end of the year (October 2016 and 2017) reaches its minimum value.

REFERENCES

[1] Almhab, A. A., & Busu, I. (2008, May). Estimation of Evapotranspiration with Modified SEBAL model using Landsat-TM and NOAA-AVHRR images in arid mountains area. In *Modeling & Simulation, 2008. AICMS 08. Second Asia International Conference on* (pp. 350-355). IEEE.

[2] Chandrapala, L., & Wimalasuriya, M. (2003). Satellite measurements supplemented with meteorological data to operationally estimate evaporation in Sri Lanka. *Agricultural water management*, *58*(2), 89-107.

[3] Kongo, V. M., & Jewitt, G. P. W. (2006). Preliminary investigation of catchment hydrology in response to agricultural water use innovations: A case study of the Potshini catchment–South Africa. *Physics and Chemistry of the Earth, Parts A/B/C*, *31*(15-16), 976-987.

[4] Tang, R., Li, Z. L., Chen, K. S., Jia, Y., Li, C., & Sun, X. (2013). Spatial-scale effect on the SEBAL model for evapotranspiration estimation using remote sensing data. *Agricultural and forest meteorology*, *174*, 28-42.

[5] Jia, L., Xi, G., Liu, S., Huang, C., Yan, Y., & Liu, G. (2009). Regional estimation of daily to annual regional evapotranspiration with MODIS data in the Yellow River Delta wetland. *Hydrology and Earth System Sciences*, *13*(10), 1775-1787.

[6] Yang, W., Shabanov, N. V., Huang, D., Wang, W., Dickinson, R. E., Nemani, R. R., ... & Myneni, R. B. (2006). Analysis of leaf area index products from combination of MODIS Terra and Aqua data. *Remote Sensing of Environment*, *104*(3), 297-312.

[7] Mokhtari, M. H. (2006). Agricultural drought impact assessment using remote sensing: a case study Borkhar district, Iran. ITC.\

[8] Bastiaanssen, W. G., Menenti, M., Feddes, R. A., & Holtslag, A. A. M. (1998). A remote sensing surface energy balance algorithm for land (SEBAL). 1. Formulation. *Journal of hydrology*, *212*, 198-212.

[9] Bastiaanssen, W. G. M., Pelgrum, H., Wang, J., Ma, Y., Moreno, J. F., Roerink, G. J., & Van der Wal, T. (1998). A remote sensing surface energy balance algorithm for land (SEBAL).: Part 2: Validation. *Journal of hydrology*, *212*, 213-229.

[10] Allen, R. G., Tasumi, M., Morse, A., Trezza, R., Wright, J. L., Bastiaanssen, W.& Robison, C. W. (2007). Satellite-based energy balance for mapping evapotranspiration with internalized calibration (METRIC)—Applications. *Journal of irrigation and drainage engineering*, *133*(4), 395-406.

[11] Almhab, A. A., & Busu, I. (2008, May). Estimation of Evapotranspiration with Modified SEBAL model using Landsat-TM and NOAA-AVHRR images in arid mountains area. In *Modeling & Simulation, 2008. AICMS 08. Second Asia International Conference on* (pp. 350-355). IEEE.

[12] Wang, X., Zhang, C., & Wei, J. (2010). Application of the SEBAL method in water resources management in the Yellow River Delta of China. *Desalination and Water Treatment*, *19*(1-3), 212-218.

[13] Bastiaanssen, W. G. M., Noordman, E. J. M., Pelgrum, H., Davids, G., Thoreson, B. P., & Allen, R. G. (2005). SEBAL model with remotely sensed data to improve water-resources management under actual field conditions. *Journal of irrigation and drainage engineering*, *131*(1), 85-93.

[14] Seyyed Hossein, S.N., N. Samira, H.N., Seyyed Majid, Estimation of Real Evapotranspiration Using Satellite Images in Mashhad.

[15] Du, J., Song, K., Wang, Z., Zhang, B., & Liu, D. (2013). Evapotranspiration estimation based on MODIS products and surface energy balance algorithms for land (SEBAL) model in Sanjiang Plain, Northeast China. *Chinese geographical science*, *23*(1), 73-91.

[16] Sun, Z., Wei, B., Su, W., Shen, W., Wang, C., You, D., & Liu, Z. (2011). Evapotranspiration estimation based on the SEBAL model in the Nansi Lake Wetland of China. *Mathematical and Computer Modelling*, *54*(3-4), 1086-1092.